JOURNAL OF GEOPHYSICAL RESEARCH, VOL. 86, NO. A7, PAGES 5438-5448, JULY 1, 1981

Coronal Streamers in the Solar Wind at 1 AU

J. T. Gosling[1], G. Borrini[2], J. R. Asbridge[1], S. J. Bame[1], W. C. Feldman[1], and R. T. Hansen[3]

Examination of solar wind plasma data obtained by the Los Alamos experiments on Imp 6, 7, and 8 during the 1971 - 1978 interval has revealed a frequent association between minimums in helium abundance and maximums in proton density. These events occur at low flow speeds and are strongly correlated with polarity reversals in the interplanetary magnetic field. A large fraction of these high proton density-low helium abundance events are examples of noncompressive density enhancements (NCDE), i.e., large positive density signals not readily associated with stream-stream interactions. The cleanest examples of these events often occur at well defined sector boundaries; complex, multiple events with 2 or more peaks in proton density and lasting ~3-7 days are, however, common, and are associated with multiple field polarity reversals. When mapped back to the sun, assuming constant speed along a stream tube, these high proton density - low helium abundance events associated with magnetic field reversals usually correspond to intersections of the spacecraft trajectory with the mid line of a coronal streamer belt that encircles the sun. The duration or multiplicity of these 1 AU events is generally correlated with the local tilt of the middle of the streamer belt to the solar equator. These events thus appear to be the 1 AU extensions of coronal streamers. A fine scale warping of the streamer belt on a longitudinal scale of ~10° and varying thickness and density of the streamer belt at 1 AU adequately account for the variety of low helium abundance - high proton density events observed. It is not yet understood why the helium abundance is low within coronal streamers at 1 AU.

1. Introduction

Substantial variations in the solar wind helium-hydrogen abundance ratio (hereafter denoted A(He)) have been reported by virtually all solar wind observing groups [e.g., *Neugebauer and Snyder*, 1966; *Robbins et al.*, 1970; *Ogilvie and Wilkerson*, 1969; *Bame*, 1972; *Bollea et al.*, 1972]. The range of reported abundance values extends from less than 0.001 to greater than 0.35 [e.g., *Feldman et al.*, 1977]. This great variability was not expected prior to the observations. Although generally attributed to some fractionation process occurring in the solar atmosphere [e.g., *Jokipii*, 1966; *Nakada*, 1969], neither the origin of this variability nor its dependence on abundance values in the lower and intermediate corona are clearly understood [e.g., *Geiss et al.*, 1970; *Joselyn and Holzer*, 1978; *Borrini and Noci*, 1979].

Nevertheless, previous experimental work has succeeded in bringing a certain degree of ordering to the observed variability. For example, within the cores of most quasi-stationary high speed streams A(He) is relatively constant with an average value of 0.048 ±0.005 [*Bame et al.*, 1977]. Periods of extremely high abundance, say ≳0.15, are generally short-lived (~1 - 15 hours duration), often follow outward propagating shocks by ~10 - 20 hours, and presumably identify material ejected into the solar wind from the lower solar atmosphere during transient solar activity [e.g., *Hirshberg et al.*, 1972*a*]. Periods of low (say < ~0.02) abundance occur preferentially at low flow speeds [e.g., *Hirshberg et al.*, 1972*b*]; in particular, a minimum in A(He) often occurs ~1/2 day prior to the onset of a high speed stream [*Hirshberg et al.*, 1974; *Gosling et al.*, 1978], and an abrupt increase in A(He) commonly is observed at the interface that separates what was originally dense slow gas from what was originally less dense fast gas at the leading edge of a high speed stream [*Gosling et al.* 1978]. On the other hand, A(He) is not uniformly low at low flow speeds; in fact, great variability of A(He) is one characteristic of low speed flows [*Bame et al.*, 1977; *Feldman et al.*, 1977]. Finally, during solar cycle 20, long-term averages of A(He) increased from ~0.03 up to ~0.05 [*Ogilvie and Hirshberg*, 1974] and decreased back to ~0.03 [*Feldman et al.*, 1978] roughly in phase with the solar activity cycle, but lagging behind by 1 - 2 years. The solar cycle effect is primarily associated with low flow speeds and/or high proton densities (*Feldman et al.*, 1978). These and other observations have recently been reviewed by *Neugebauer* [1980].

One of the difficulties associated with achieving an understanding of A(He) variability is that the solar origin of low speed flows, where much of the A(He) variability occurs, is uncertain. In fact, the overall variability of the low-speed solar wind [*Bame et al.*, 1977; *Feldman et al.*, 1977] suggests that either more than one solar source is involved in producing low speed flows, or that the source is intrinsically time variable or strongly structured spatially, or all three.

With the dual hope of (1) achieving a better understanding of the manner in which solar wind A(He) variability is organized and (2) identifying the solar origin of low-speed flows, we recently undertook a study of Los Alamos Imp solar wind data obtained between March 1971 and December 1978. This examination of the Imp data has revealed an association between low A(He) and high

[1]University of California, Los Alamos National Laboratory, Los Alamos, New Mexico 87545.
[2]Institute for Plasma Research, Stanford University, Stanford, California 94305.
[3]Veterans Administration Medical Center, West Haven, Connecticut 06516.

Paper number 1 A0003.
0148-0227/81/001A-0003$01.00

proton density that occurs at low flow speeds and that is correlated with polarity reversals of the interplanetary magnetic field. The nature of this association has been documented [*Borrini et al.*, 1981] by performing a superposed epoch analysis on the Imp data using as the key times or zero epochs an independently selected subclass of field reversal events - 'well-defined sector boundary crossings' [e.g., *Wilcox and Ness*, 1965]. This analysis demonstrated the coupled variation in solar wind A(He), proton density, temperature, and flow speed often found near field polarity reversals. Previous work indicates that well defined sector boundaries are the 1 AU extensions of a neutral line or current sheet that encircles the sun and above which lies an extended band of enhanced coronal brightness [*Schulz*, 1973; *Hansen et al.*, 1974; *Howard and Koomen*, 1974; *Svalgaard et al.*, 1974; *Korzhov*, 1977; *Hundhausen*, 1977; *Pneuman et al.*, 1978]. The coupled variations discussed by *Borrini et al.* [1980] are thus believed to be a 1 AU 'signal' of the plasma surrounding the current sheet.

As was noted above, the flow pattern discussed by Borrini et al. is a common feature of the low speed solar wind near interplanetary magnetic field polarity reversals, even near those many reversals that do not qualify as well defined sector boundaries. Our purpose here is to (1) present further examples of the low A(He), high proton density, low speed, magnetic field polarity association, (2) document the common occurrence of multiple events lasting ~3 - 7 days, and (3) present the results of our attempts to relate these events directly to maps or isophotes of solar coronal brightness at 1.5 solar radii (R_s). This study suggests that a substantial fraction of the low-speed solar wind originates in coronal streamers, particularly near solar minimum. For as yet unspecified reasons, A(He) is low within coronal streamers in the solar wind at 1 AU (see, however, *Borrini et al.* [1980] for a possible explanation).

2. The Data Sets

The Los Alamos solar wind ion experiments on Imp 6, 7, and 8 are similar in design and are narrow gap ($\Delta r/R \sim 0.04$) spherical section electrostatic analyzers with bending angles ≥160° each followed by a high-efficiency electron multiplier. Plate voltages are swept to obtain energy/charge (E/Q) spectra over the range 125 - 5157 eV in the case of Imp 6 and 165 - 9294 eV in the cases of Imp 7 and 8. In these spectra, He^{++} appears at approximately twice the E/Q value of H^+. Normally, the ion kinetic temperature is sufficiently low that He^{++} and H^+ are clearly separated in the Imp data. Times when this criterion is not satisfied have been eliminated from the He^{++} data set (less than 15% of the potential He^{++} data set has been so eliminated). This selection criterion results in a scarcity of He^{++} measurements on the leading edges of high speed streams where the temperature is high and the speed is relatively low. The data to be shown in this paper are 1-hour averages of individual measurements normally obtained once every ~2 min. A(He) values plotted and quoted herein correspond to the ratio of the He^{++} flux to the H^+ flux. This definition has the virtue that A(He) remains constant with heliocentric distance as plasma moves outward along a flux tube. Because H^+ and He^{++} bulk flow speeds at 1 AU seldom differ from one another by more than 10%, the flux ratio is, to a good approximation, the same as the number density ratio. Further information on the instruments and the data reduction procedures can be found in previous publications [e.g., *Feldman et al.*, 1973; *Asbridge et al.*, 1976; *Feldman et al.*, 1976; *Bame et al.*, 1977].

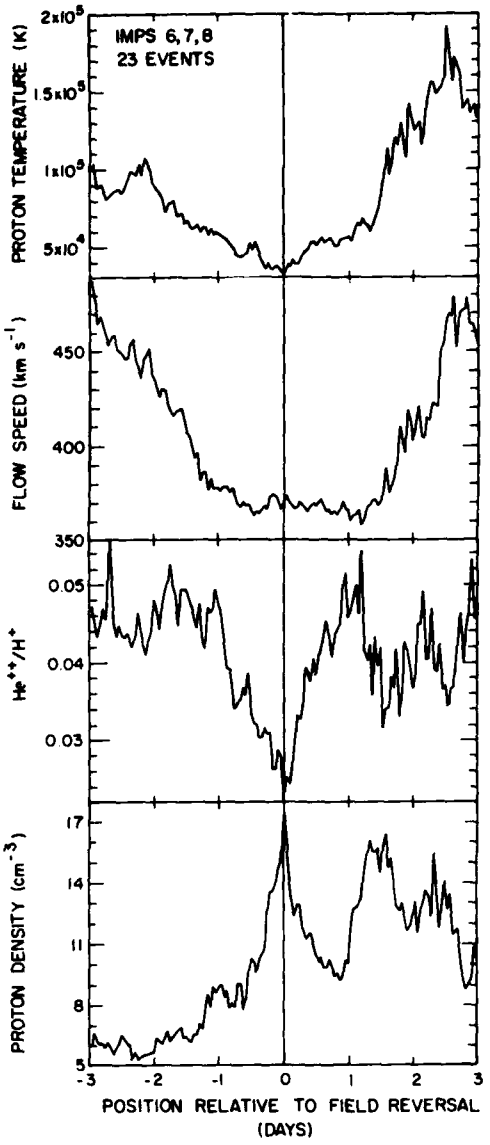

Fig. 1. Superposed epoch plots of the solar wind proton density, helium abundance, flow speed, and proton temperature for 23 well-defined sector boundaries more than one day removed from speed rises associated with high-speed streams. One-hour averages are employed, and sector boundary passage was used as zero epoch. The well-developed minimums in abundance, flow speed, and proton temperature, and maximum in proton density are characteristic near field reversals. Adapted from *Borrini et al.* [1981].

The data on the white light corona were obtained with a K coronameter operated by the High Altitude Observatory in Hawaii. This instrument scans the polarization

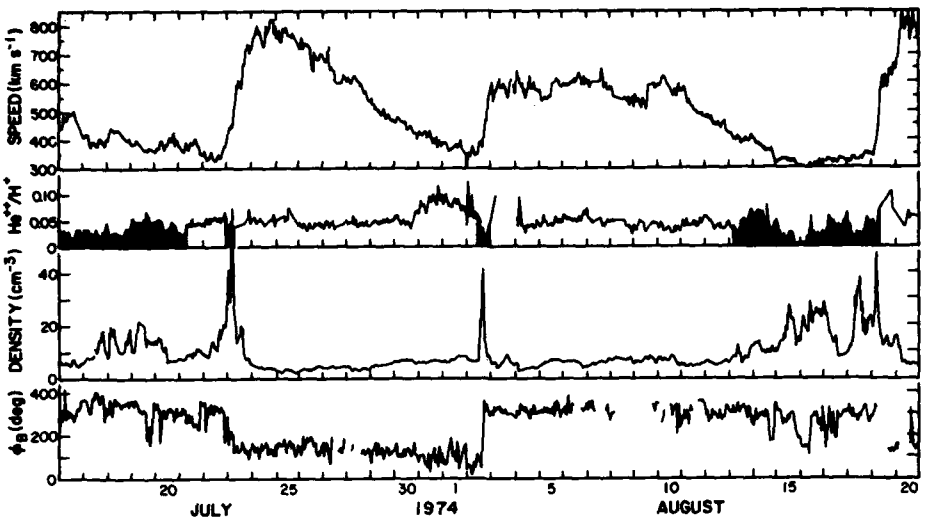

Fig. 2. Solar wind flow speed, helium abundance, and proton density as determined by Los Alamos instruments on Imp 6, 7, and 8 together with the magnetic field azimuth during July and August 1974. The shading under the He^{++}/H^{+} trace indicates intervals of generally low A(He) associated with low flow speeds, high proton density, and field polarity reversals. These intervals map into the vertically shaded solar longitudes of Figure 3.

brightness pB (the difference in the intensity of white light coronal radiation polarized along the direction radial to the sun and that radiation polarized transverse to the radial direction) at 5° intervals around the occulted limb of the sun at a series of heights between 1 and 16 min of arc above the limb. Details of the instruments and the resulting data can be found elsewhere [*Wlérick and Axtell*, 1957; *Hansen et al.*, 1969*a*, *b*]. Sequences of data from daily scans are combined to form synoptic maps or contours of pB as a function of solar latitude and longitude. The synoptic maps displayed in this paper pertain to a height of 1.5 R_s from sun center and were derived from east limb measurements except where indicated on the figures. A recent and thorough discussion of this display technique, its limitations, and interpretations in terms of coronal electron density is given by *Hundhausen et al.* [1981].

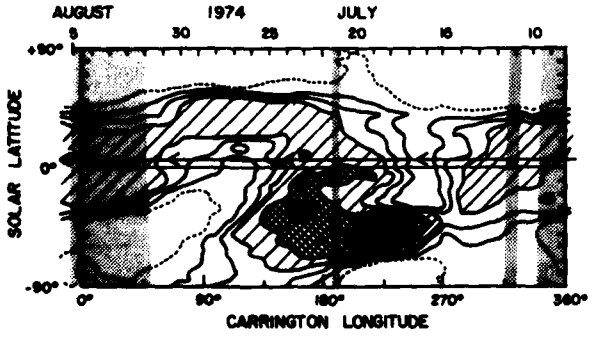

Fig. 3. Contour maps of coronal brightness (pB) as a function of solar latitude and Carrington longitude. These maps are derived from daily observations of pB at a height of 0.5 solar radii above the east limb. The date of east limb measurement is indicated at the top of the figure. Contours correspond to pB values of 1, 2, 3, 4, 6, 8 and 10 × 10^{-6} the brightness of the solar disk. The dotted curve is the 1 × 10^{-6} contour; increasingly darker shadings denote increasingly brighter corona. The arrowed line traces the spacecraft trajectory; vertical shadings indicate the mapped longitudes for the low A(He) events selected in Figure 2.

3. The Observations

Figure 1 presents a limited portion of the results of the superposed epoch analysis described by *Borrini et al.* [1981]. Zero epoch in the particular analysis shown was a set of 23 'well-defined sector boundaries' that were not followed within 1 day by a rise in solar wind speed. The latter restriction was incorporated to minimize distortions of the sector boundary signal caused by streamline compression in interplanetary space [e.g., *Gosling et al.*, 1972]. It should be emphasized that the coincidence of extremums in A(He), solar wind speed, proton temperature, and proton density with the field reversal is an average effect not always exhibited by individual events included in the sector boundary study. In fact, not only do these extremums frequently occur a number of hours before or after the field reversal in individual events, but also the various extremes frequently do not occur simultaneously. Nevertheless, the general correspondence of minimums in A(He), solar wind speed, and proton temperature, with a maximum in proton density and with sector boundary passage is an accurate representation of solar wind variations observed near sector boundaries.

A major point we wish to make is that this same general pattern is a common feature of the Los Alamos Imp data when the flow speed is low, even when the field polarity reversals do not qualify as well defined sector boundaries. This point is well illustrated by the data string plotted in Figure 2. Shown there are 1-hour averages of solar wind speed, A(He), proton density, and the azimuthal angle of the interplanetary magnetic field ϕ_B (obtained from *King*, [1977, 1979]), as a function of time in July and August 1974. A well defined sector boundary was observed late in the day on August 2; the accompanying minimums in A(He) and flow speed and maximum in proton density provide a classic example of the signature of these boundaries. Note, however, the elevated values of A(He) (~0.08) that existed for a couple of days prior to boundary passage. Such elevations in A(He) are not uncommon in

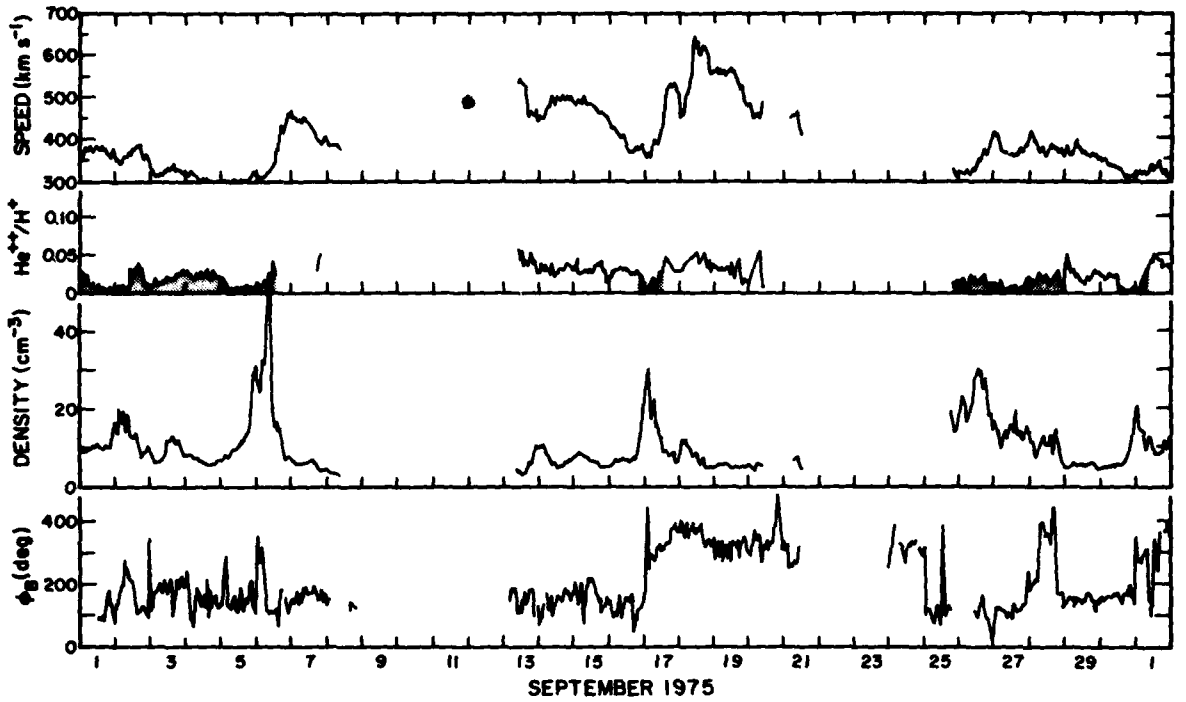

Fig. 4. Solar wind data obtained in September 1975. The format is identical to Figure 2.

the low speed solar wind, do not have any obvious association with field polarity reversals, and are presently of unknown origin. Of more immediate interest to the present paper are the multiple proton density peaks in the July 17 - 23 and August 13 - 19 intervals, which have a general, but loose, correlation with field polarity reversals, low A(He), and low solar wind speed. Careful examination of these intervals reveals a number of distinct anticorrelations of proton density and A(He), while the association with specific field polarity reversals is less well defined. This type of association is representative of what was observed during the approach to and near solar minimum (1972 - 1977). In 1971 and 1978, high proton densities and low speeds and temperatures were found near field polarity reversals, but the low A(He) signal was often absent. On the other hand, in all years very low A(He) events had a strong association with field polarity reversals (see Table 1).

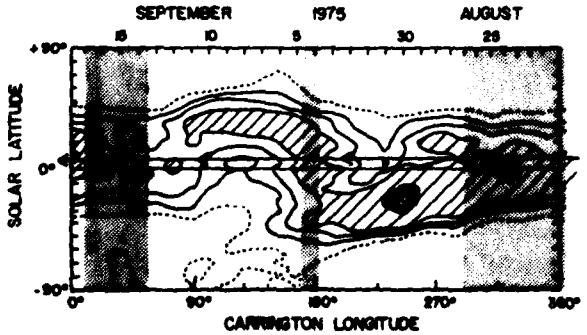

Fig. 5. Contour maps of coronal brightness, as in Figure 3. The shaded intervals in Figure 4 map into the longitudes indicated by the vertical shadings in this figure.

The shading beneath the A(He) trace in Figure 2 is meant to emphasize those intervals of predominantly low A(He) having the general characteristics outlined above. We have performed a mapping of these data intervals back to the vicinity of the sun by assuming that the flow speed is constant at all heliocentric distances on a given stream tube. Although difficult to justify theoretically (see, however, *Nolte and Roelof* [1973*a*, *b*]), this same approximation of constant speed has been used successfully to identify unipolar regions [*Hundhausen*, 1972] and coronal holes [e.g., *Krieger et al.*, 1973; *Hundhausen*, 1977] as the source of high speed solar wind streams. The intervals indicated by shading in Figure 2 map back to the longitudinal intervals indicated by the vertical shadings in Figure 3. These shadings in Figure 3 are superposed upon contours of coronal white light pB measured at a height of 1.5 R_s from the center of the sun (0.5 R_s above the limb). Carrington longitude runs from left to right in Figure 3; the date of measurement above the east limb runs from right to left and is indicated at the top of the plot. Time delays of 11 - 12 days typically are involved between the date of measurement of coronal pB at the east limb and measurement of low A(He) in the solar wind at 1 AU (~6.8 days for rotation from the limb to central meridian and ~5 days out to 1 AU). The spacecraft trajectory (at 1 AU) is indicated by the arrowed line running nearly parallel to the solar equator.

Perhaps the most obvious coronal feature in Figure 3 is a belt of coronal brightness that encircles the sun at low solar latitudes, but that is skewed relative to the solar equator. Considerable evidence suggests that this band of coronal brightness (hereafter called the streamer belt) lies above a neutral line separating hemispheres of opposite magnetic polarity (see the references quoted in the in-

troduction); the dominant cause of the skewness is thought to be an ~30° tilt of the solar dipole to the axis of solar rotation at this phase of the solar activity cycle (see, for example, the review by *Hundhausen* [1977]). Intersections of the spacecraft trajectory with the mid line of the streamer belt coincide with our selected high proton density and low A(He) events. Further, the duration or multiplicity of the events appears to be correlated with the local tilt of the middle of the belt relative to the spacecraft trajectory (or, nearly equivalently, the solar equator). For example, the brief low A(He) event observed at 1 AU on August 2 in association with a well-defined sector boundary crossing maps back to Carrington longitude ~190°, at which point the middle of the streamer belt is aligned almost perpendicular to the spacecraft trajectory. On the other hand, the multiple events observed in the July 17 - 23 and August 13 - 19 intervals at 1 AU map back to Carrington longitudes 315° - >360° and <0° - 50°, respectively, where the middle of the streamer belt locally is nearly parallel to and at the same latitude as the spacecraft trajectory. Although there is a general association of high solar wind density with these intersections with the middle of the streamer belt, the magnitude of any particular solar wind density peak in Figure 2 is not easily predicted from the 1.5 R_s coronal brightness isophotes of Figure 3.

Figure 4 displays solar wind data obtained in September 1975, approximately 13 months after the data of Figure 2. The high speed streams in the ecliptic plane at this time were less well developed than in July-August 1974, and our temporal coverage of the 1 AU solar wind was less complete. Nevertheless, several good examples of low A(He), low flow speed, and high proton density found in association with field polarity reversals can be seen in the data. These examples include a brief (~1 day) event centered on a relatively clean field reversal on September 17 that exhibits the simple pattern illustrated in Figure 1. In addition, multiple density peaks and A(He) minimums were observed in the low-speed flows of September 1 - 6 and September 25 - October 1 in loose association with multiple interplanetary magnetic field polarity reversals. These events have been mapped back to the sun in the same manner as previously described and the results are shown in Figure 5. As noted elsewhere [*Hundhausen et al.*, 1981], the streamer belt at this time had much the same appearance as in mid 1974, although the skewing of the belt relative to the solar equator was noticeably less. The same general correlations exist between intersections of the spacecraft trajectory with the middle of the streamer belt and the high proton density and low A(He) events at 1 AU as in the 1974 data. In particular, the brief, relatively clean field reversal event of September 17 (Figure 4) maps back to Carrington longitude ~180° where the spacecraft trajectory intersects the middle of the streamer belt at a steep angle. Likewise, the multiple events observed in the September 1 - 6 and September 25 - October 1 intervals map to Carrington longitudes 290° - >360° and <0° - 55°, respectively, where the middle of the streamer belt locally is at the same latitude as the spacecraft trajectory and is oriented nearly parallel to it. Again, although the 1 AU densities are generally high where the trajectory intersects the middle of the streamer belt, individual peaks in the 1 AU densities do not appear to be correlated with individual peaks in coronal brightness (density) at 1.5 R_s.

As a final illustration of these effects, Figures 6 and 7 show solar wind and coronal data for the next solar rotation. Examples of low A(He), low flow speed, and high proton density occur in association with field polarity

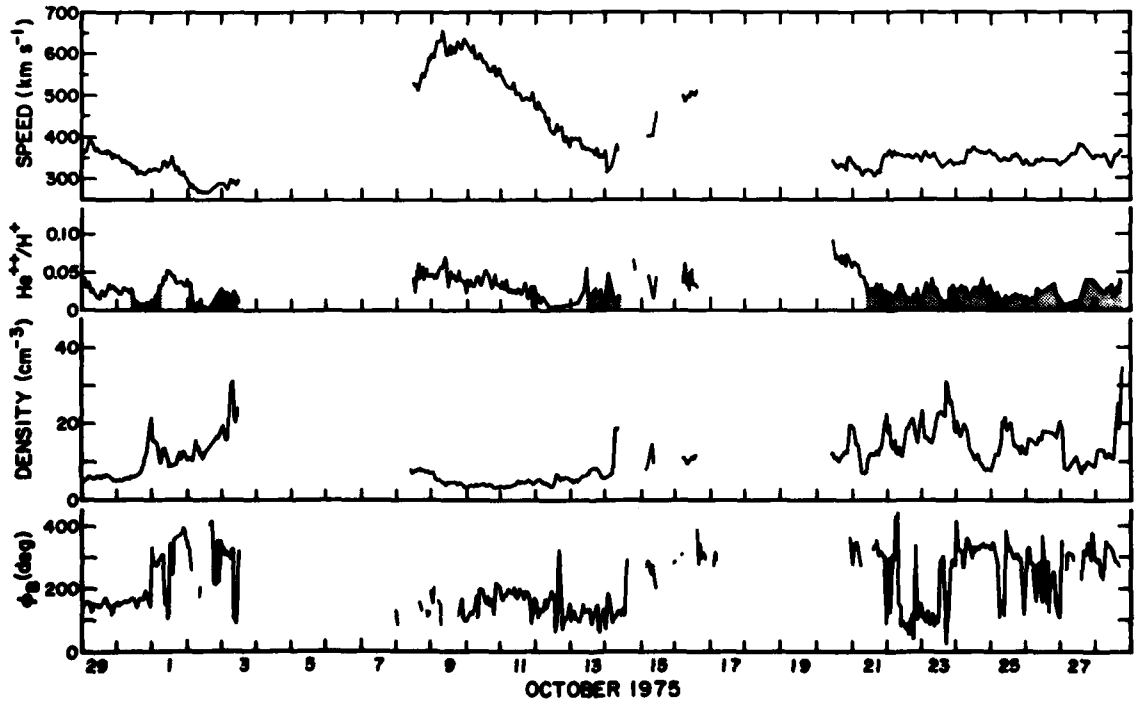

Fig. 6. Solar wind data obtained in October 1975 and displayed in a format identical to Figure 2.

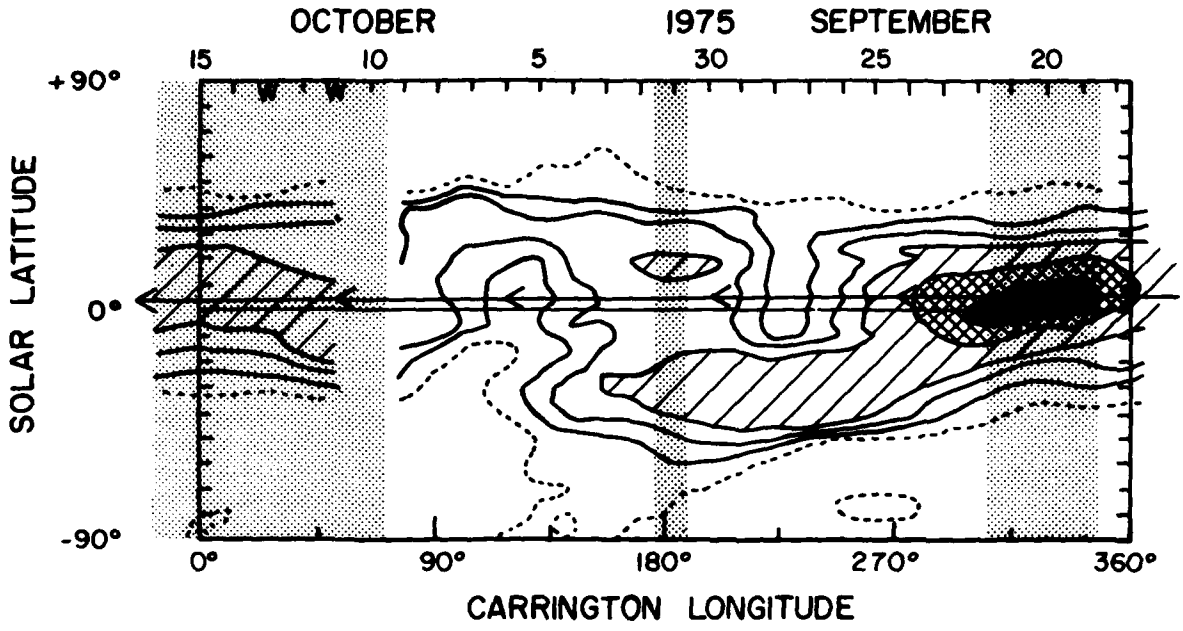

Fig. 7. Contour maps of coronal brightness, as in Figure 3. The W's near the upper left indicate the use of west limb measurements to derive the isophotes at those particular longitudes. The shaded intervals in Figure 6 map into the longitudes indicated by the vertical shadings in this figure.

reversals on October 14 and in the September 30 - October 3 and October 21 - 27 intervals. (An additional low A(He) event occurs near a brief polarity reversal on October 12, but the proton density at that time was not elevated.) The shadings in Figure 7 indicate the respective Carrington longitudes to which these events map. Multiple events in the September 30 - October 3 and October 21 - 27 intervals map back to Carrington longitudes 305 - 350° and <0° - 70°, respectively, and correspond to spacecraft intersections with the middle of the streamer belt where the mid line of the belt nearly parallels the spacecraft trajectory. The relatively narrow event on October 13 - 14 maps back to Carrington longitude 180° and corresponds to an intersection with the middle of the streamer belt where the belt is nearly perpendicular to the spacecraft trajectory. (The October 12 event maps back to nearly this same Carrington longitude because of its higher speed.) Note that the 1 AU proton densities in the September 30 - October 3 interval are not higher than those in the October 21 - 27 interval even though the former events result from an intersection with an exceptionally bright portion of the streamer belt at 1.5 R_s.

4. Observational Summary

In the previous section data from three separate solar rotations during 1974 and 1975 were presented in order to illustrate certain aspects of the low speed solar wind. The important results are summarized briefly below.

1. A general association exists between low solar wind speeds, low A(He), high proton density, and polarity reversals in the interplanetary magnetic field. The cleanest examples of this correlation often occur near well defined sector boundaries [see *Borrini et al.*, 1981].

2. Complex, multiple events with the above characteristics and lasting for ~3 - 7 days are common, particlarly near solar minimum.

3. When mapped back to the sun assuming constant speed along a stream tube, it is found that these low A(He) - high proton density events tend to occur at intersections of the spacecraft trajectory with the mid line of a streamer belt (neutral line) that encircles the sun.

4. Multiple events usually correspond to intersections where the middle of the streamer belt nearly parallels the spacecraft trajectory, and briefer events (~1 day duration) usually correspond to intersections where the middle of the streamer belt is highly tilted with respect to the spacecraft trajectory.

The 1974 - 1975 interval is particularly useful for displaying the above noted effects because the streamer belt at that time was highly skewed with respect to the solar equator. Further, the corona [*Hansen et al.*, 1976; *Hundhausen et al.*, 1981] and the solar wind [*Gosling et al.*, 1976; *Feldman et al.*, 1978] were both relatively stable from one solar rotation to the next. Such a situation did not prevail throughout the entire interval studied. For example, during 1976 and 1977 much of the belt was aligned nearly parallel to the solar equator [*Hundhausen et al.*, 1981] and multiple events lasting 3 - 7 days were more common. Nevertheless, our mapping result is a general one: Throughout the interval studied multiple occurrences of the low A(He), high density, field polarity reversal pattern usually correspond to spacecraft orbit intersections with the middle of the streamer belt at longitudes where the middle of the belt is aligned nearly parallel to the orbit, and more sharply delineated events usually correspond to intersections at longitudes where the middle of the belt is significantly inclined to the spacecraft orbit. Exceptions to this rule occur of course. It appears these exceptions can be explained in terms of a warping of the

streamer belt on a longitudinal scale of ~10° (see the discussion section).

Some further qualifications to the results summarized above are worth mentioning. First, as noted by *Borrini et al.* [1981], in 1971 and 1978 many polarity reversals and intervals of high density were not accompanied by low A(He). That is, the pattern we have been discussing was more commonly observed during the approach to and near solar minimum than near solar maximum. In fact, in 1971 and 1978 enhancements in A(He) often accompany proton density peaks and field reversals. It is this difference in behavior at different phases of the solar cycle that accounts for the overall decline in average A(He) with declining solar activity [*Feldman et al.*, 1978]. Second, even near solar minimum neither all periods of low flow speed nor all periods of depressed A(He) fit conveniently into the pattern we have described. However, a substantial fraction do. For example, Tables 1 and 2, which present the results of a statistical study of all events with A(He) ≤ 0.015, illustrate that such intervals preferentially occur at low flow speeds near field polarity reversals. On the other hand, only a little more than half of these very low A(He) events are associated with proton densities >12 cm^{-3}. (In constructing Tables 1 and 2, the multiple type events we have described were considered single events; a field reversal was considered to be associated with the event if the reversal occurred within ±12 hours of A(He) ≤ 0.015.)

Finally, our mapping procedure is based upon two assumptions: (1) The corona remains relatively constant for the ~6.8 days required for rotation from the east limb to central meridian, and (2) 1 AU data can be projected back to the sun simply by assuming constant speed on a stream tube at all heliocentric distances. The latter assumption particularly is difficult to justify. It does, however, provide results that are consistent and that have a straightforward interpretation.

5. Discussion

We have succeeded in identifying a characteristic solar wind flow pattern associated with many intervals of depressed He^{++} abundance (A(He)). The analysis of *Borrini et al.* [1981] establishes the correlation of this pattern with polarity reversals in the interplanetary magnetic field. The close correlation of this flow pattern with field reversals and the consistent mapping of this flow pattern back to the coronal streamer belt indicate that the pattern is a signal of the coronal streamer belt at 1 AU. Measurements of the solar wind oxygen ionization temperature when the low A(He) pattern is present provide further support for this interpretation [*Feldman et al.*, 1981]. These ionization temperatures (~ 2×10^6 K), which correspond to the electron temperature at ~$2R_s$ from sun center, match temperatures of streamers inferred from line profile analyses and density scale height determinations.

We should not be surprised that the signal of a coronal streamer at 1 AU includes a high density, for high density is the essence of coronal streamers in, for example, eclipse photographs. (Following *Newkirk* [1967], we define streamers to be the large structures, often helmet-like in appearance, which are brighter than the background corona and which extend outward beyond 1.5 - 2.0 R_s from sun center.) However, large density signals are also produced in interplanetary space by the steepening of high-speed streams [e.g., *Carovillano and Siscoe*, 1969; *Hundhausen*, 1973], and it is not always a simple task to separate density signals of essentially interplanetary origin from those of essentially coronal origin. In a similar fashion, interplanetary dynamics probably also causes some dense coronal structures to map into 1 AU flows which have only average densities. Nevertheless, results of several previous studies [e.g., *Belcher and Davis*, 1971; *Gosling et al.*, 1972, 1978; *Rosenbauer et al.*, 1977] have also led to the interpretation that at least some of the high densities observed between high speed streams are essentially of coronal origin.

Figure 8 provides an idealized schematic view of a cross-section of the streamer belt. The particular view illustrated corresponds to a cut through the belt at a longitude where the belt is inclined perpendicular to the solar equator (e.g., Carrington longitude 190° in Figure 3). Although the figure exhibits a certain degree of symmetry about the central longitude, real streamers need not and, in fact, often do not exhibit such symmetry. Effects of solar rotation are neglected. The figure emphasizes the following characteristics of streamers as inferred from both 1 AU measurements of the solar wind and eclipse and coronagraph observations.

1. Streamers have a higher density than their sur-

Table 1. Percentages of Very Low Helium Abundance (A(He) ≤ 0.015) Events Associated With Field Polarity Reversals, High Proton Density (n_p > 12 cm^{-3}), and Low Flow Speed (v < 450 km s^{-1})

Year	Events	Reversals	High Density	Low Speed
1971	7	86%	43%	86%
1972	25	83%	56%	96%
1973	30	79%	57%	77%
1974	27	58%	63%	82%
1975	45	70%	62%	71%
1976	49	78%	84%	90%
1977	54	83%	65%	87%
1978	40	71%	43%	73%
All years combined	277	75%	62%	82%

Field data are not available for all of the events listed in the second column. The percentages in the third column are based on events where field data are available.

Table 2. Joint Percentages of Very Low Helium Abundance (A(He) ≤ 0.015) Events Associated With Field Polarity Reversals, High Proton Density (n_p > 12 cm^{-3}), and Low Flow Speed (v < 450 km s^{-1})

Year	Reversals, High Density	Reversals, Low Speed	High Density, Low Speed	Reversals, High Density, Low Speed
1971	43%	71%	43%	43%
1972	57%	83%	56%	52%
1973	57%	68%	57%	57%
1974	50%	58%	63%	50%
1975	60%	68%	60%	60%
1976	70%	73%	82%	70%
1977	58%	78%	63%	56%
1978	57%	64%	35%	50%
All years combined	59%	71%	60%	58%

Field data are available for only 77% of the events studied; the percentages tabulated are normalized accordingly.

roundings at all heliocentric distances. The density is greatest on closed field lines [e.g., *Pneuman*, 1973].

2. A field polarity reversal usually occurs near the middle of a streamer.

3. Streamers neck down with increasing height above the limb. Because of this a streamer's angular cross section as measured from sun center decreases with increasing heliocentric distances.

4. Closed field lines indicate where the coronal plasma is constrained from expanding outward [e.g., *Pneuman and Kopp*, 1971]. On open field lines within the streamer the expansion of the coronal plasma proceeds at a lower speed than outside the streamer. (This is inferred from our measurements and predicted, for example, by *Pneuman and Kopp* [1971].) The outer edges of streamers may be the sites of shears in the flow [*Gosling et al.*, 1978].

5. A(He) is generally low within a streamer at 1 AU and presumably closer to the sun as well where the abundance freezes in. *Borrini et al.* [1981] suggest that low A(He) within streamers may be a result of gravitational stratification in the solar atmosphere combined with a relatively distant sonic (critical) point in streamers.

The idealized streamer sketched in Figure 8 is but one special portion of a streamer belt that, at least in the 1973 - 1977 interval, encircled the sun. Figure 9 illustrates in a schematic fashion how this streamer belt might map out to

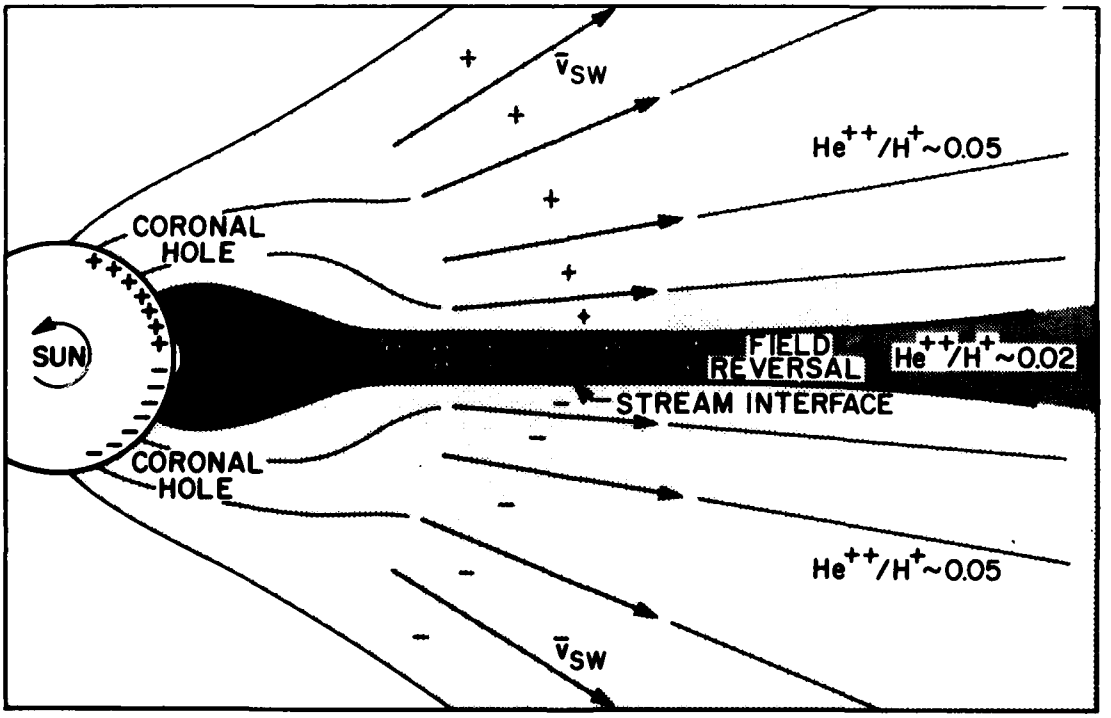

Fig. 8. An idealized schematic view of the intersection of the streamer belt with the solar equator at a longitude where the center of the belt is perpendicular to the equator. Plasma within the streamer is denser, flows slower, and has a lower helium abundance than plasma outside the streamer. The very steep radial gradient of coronal density at all longitudes is masked as if by a radially graded filter. All effects of solar rotation are neglected.

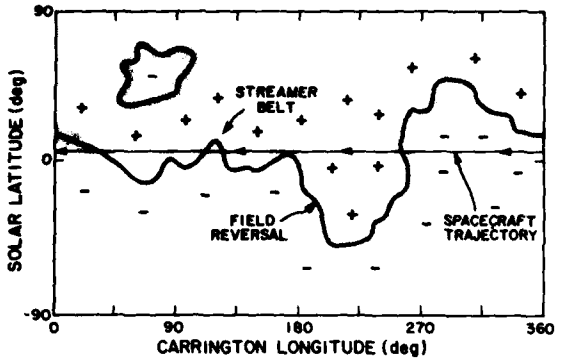

Fig. 9. Idealized schematic of the intersection of the streamer belt with the 1 AU sphere. The width and density of the belt are probably more variable than shown. In addition to the streamer belt, there probably exist streamers such as those appearing between 45° and 90° Carrington longitude that do not encircle the sun.

the 1 AU sphere and how the Imp spacecraft might intersect it during one solar rotation. In addition to the general skewing of the belt relative to the solar equator, the belt is drawn with a number of smaller warps with a scale size of ~10°. Such warping is suggested by Hα pictures of the sun underlying the corona (see, for example, *McIntosh* [1972]) and is consistent with a recent interpretation of Helios interplanetary field measurements [*Villante et al.*, 1979]. (Line of sight problems, the relatively coarse resolution of the K coronameter observations (5° in latitude and ~13° in longitude) and the fact that the coronameter measurements are at a relatively low height probably explain why this fine scale warping is not obvious in the coronal data displayed in Figures 3, 5, and 7.) The streamer belt drawn in Figure 9 straddles a region of field reversal (current sheet) that also encircles the sun much in the manner first described by *Schulz* [1973] and later elaborated upon by many authors [e.g., *Smith et al.*, 1978; *Klein and Burlaga*, 1980; *Rosenberg and Coleman*, 1980; *Wilcox et al.*, 1980]. At 1 AU our measurements suggest that the thickness of the streamer belt (i.e., its angular cross section as measured from sun center) is considerably less than at 1.5 R_s. One should not infer from Figure 9 that either the thickness or the intensity (density) of the belt is necessarily uniform with longitude. Finally, in addition to the streamer belt, Figure 9 includes an example of an isolated streamer feature above a closed loop that does not encircle the sun (see, for example, *Pneuman et al.*, [1978]).

Several types of spacecraft intersections with the streamer belt are shown in Figure 9. The crossing at Carrington longitude ~255° occurs where the belt is nearly perpendicular to the spacecraft trajectory and would correspond to a 'well-defined sector boundary.' Multiple encounters with the belt occur between Carrington longitudes 20° and 180°. No field reversals would be observed for the encounters near 80° and 170° because the spacecraft orbit never actually crosses the middle of the belt there, whereas two reversals would be observed during the encounter at ~120°. All of these encounters would, however, provide local maximums in particle density and local minimums in flow speed and helium abundance. The encounter near ~30° might be interpreted a a 'well-defined sector boundary,' but would likely be somewhat broader in extent than the crossing near 255° for equal thickness of the belt. It should be apparent that the solar wind observations presented in this paper are qualitatively consistent with the streamer belt - spacecraft intersection model sketched above. We also expect closed loop structures such as the one between 45° and 90° longitude in Figure 9 to contribute to the actual observations when these structures intersect the spacecraft trajectory, that is when they occur at low solar latitudes.

A large fraction of the individual proton density peaks associated with low A(He) and field polarity reversals are examples of what have previously been labeled noncompressive density enhancements (NCDE), i.e., density enhancements that do not obviously result from stream steepening in interplanetary space [*Gosling et al.*, 1977]. In that paper, which concentrated on Imp observations prior to August 1974, it was suggested that some NCDE's might originate in transient processes in the solar atmosphere. Subsequently, it was found that the occurrence frequency of NCDE's did not decrease with decreasing solar activity [*Feldman et al.*, 1978]. These authors suggested it was therefore unlikely that all NCDE's are caused by coronal transients. However, the solar cycle dependence of coronal transients, particularly those associated with eruptive prominences (filaments), has not yet been established, and ionization temperature measurements within NCDE's clearly suggest that at least some NCDE's originate in solar activity [*Fenimore*, 1980]. We have previously noted in this paper that during 1971 and 1978 a number of density peaks and field reversals were associated with maximums rather than minimums in A(He). Our current interpretation of NCDE's is that near solar maximum NCDE's originate in solar activity (hence the high A(He), whereas near solar minimum most NCDE's are associated with the streamer belt upon which this paper has concentrated. This suggested correlation would account in a natural way for the observed decrease in A(He) [*Feldman et al.*, 1978] with decreasing solar activity.

Acknowledgments The Los Alamos solar wind data were obtained from the Imp program of the U. S. National Aeronautics and Space Administration (NASA). Work at Los Alamos was performed under the auspices of the U. S. Department of Energy and was supported in part by NASA. The work at Stanford University has been supported by a fellowship grant from the European Space Agency and in part by the Office of Naval Research under contract N00014-76-C-0207, by the National Aeronautics and Space Administration under grant NGR 05-020-559 and contract NAS5-24420, by the Division of Atmospheric Sciences, Solar Terrestrial Research Program of the National Science Foundation under grant ATM80-20421, and by the Max C. Fleischmann Foundation. The K coronameter observations were obtained as a part of a long-term observing program conducted by the High Altitude Observatory of Boulder, Colorado, and was funded by the National Science Foundation.

The Editor thanks V. J. Pizzo for his assistance in evaluating this paper.

References

Asbridge, J. R., S. J. Bame, W. C. Feldman, and M. D. Montgomery, Helium and hydrogen velocity differences in the solar wind, *J. Geophys. Res.*, *81*, 2719, 1976.

Bame, S. J., Spacecraft observations of the solar wind composi-

tion, in *Solar Wind*, edited by P. J. Coleman, C. P. Sonett, and J. M. Wilcox, *NASA SP-308*, p. 535, Washington D. C., 1972.

Bame, S. J., J. R. Asbridge, W. C. Feldman, and J. T. Gosling, Evidence for a structure-free state at high solar wind speeds, *J. Geophys. Res.*, *82*, 1487, 1977.

Belcher, J. W., and L. Davis, Jr., Large-amplitude Alfvén waves in the interplanetary medium, 2, *J. Geophys. Res.*, *76*, 3534, 1971.

Bollea, D., V. Formisano, P. C. Hedgecock, G. Moreno, and F. Palmiotto, Heos 1 helium observations in the solar wind, in *Solar Wind*, edited by P. J. Coleman, C. P. Sonett, and J. M. Wilcox, *NASA SP-308*, p. 588, Washington D. C., 1972.

Borrini, G., and G. Noci, Dynamics and abundance of ions in coronal holes, *Solar Phys.*, *64*, 367, 1979.

Borrini, G., J. T. Gosling, S. J. Bame, W. C. Feldman, and J. M. Wilcox, Solar wind helium and hydrogen structure near the heliospheric current sheet - A signal of coronal streamers at 1 AU, *J. Geophys. Res.*, *86*, in press, 1981.

Carovillano, R. L., and G. L. Siscoe, Corotating structure in the solar wind, *Solar Phys.*, *8*, 401, 1969.

Feldman, W. C., J. R. Asbridge, and M. D. Montgomery, Double ion streams in the solar wind, *J. Geophys. Res.*, *78*, 2017, 1973.

Feldman, W. C., J. R. Asbridge, S. J. Bame, and J. T. Gosling, High-speed solar wind flow parameters at 1 AU, *J. Geophys. Res.*, *81*, 5054, 1976.

Feldman, W. C., J. R. Asbridge, S. J. Bame, and J. T. Gosling, Plasma and magnetic fields from the sun, in *The Solar Output and its Variation*, edited by O. R. White, p. 351, Colorado Associated University Press, Boulder, Colorado, 1977.

Feldman, W. C., J. R. Asbridge, S. J. Bame, and J. T. Gosling, Long-term variations of selected solar wind properties: Imp 6, 7, and 8 results, *J. Geophys. Res.*, *83*, 2177, 1978.

Feldman, W. C., J. R. Asbridge, S. J. Bame, E. E. Fenimore, and J. T. Gosling, The solar origins of solar wind interstream flows: Near-equatorial coronal streamers, *J. Geophys. Res.*, *86*, in press, 1981.

Fenimore, E. E., Solar wind flows associated with hot heavy ions, *Astrophys. J.*, *235*, 245, 1980.

Geiss, J., P. Hirt, and H. Leutwyler, On acceleration and ions in corona and solar wind, *Solar Phys.*, *12*, 458, 1970.

Gosling, J. T., A. J. Hundhausen, V. Pizzo, and J. R. Asbridge, Compressions and rarefactions in the solar wind: Vela 3, *J. Geophys. Res.*, *77*, 5442, 1972.

Gosling, J. T., J. R. Asbridge, S. J. Bame, and W. C. Feldman, Solar wind speed variations: 1962 - 1974, *J. Geophys. Res.*, *81*, 5061, 1976.

Gosling, J. T., E. Hildner, J. R. Asbridge, S. J. Bame, and W. C. Feldman, Noncompressive density enhancements in the solar wind, *J. Geophys. Res.*, *82*, 5005, 1977.

Gosling, J. T., J. R. Asbridge, S. J. Bame, and W. C. Feldman, Solar wind stream interfaces, *J. Geophys. Res.*, *83*, 1401, 1978.

Hansen, R. T., S. F. Hansen, and H. G. Loomis, Differential rotation of the solar electron corona, *Solar Phys.*, *10*, 135 1969*a*.

Hansen, R. T., C. J. Garcia, S. F. Hansen, and H. G. Loomis, Brightness variations of the white-light corona during the years 1964 - 1967, *Solar Phys.*, *7*, 417, 1969*b*.

Hansen, R. T., S. F. Hansen, and C. Sawyer, Long-lived coronal structures and recurrent geomagnetic patterns in 1974, *Planet. Space Sci.*, *24*, 381, 1976.

Hansen, S. F., C. Sawyer, and R. T. Hansen, K corona and magnetic sector boundaries, *Geophys. Res. Lett.*, *1*, 13, 1974.

Hirshberg, J., S. J. Bame, and D.. E. Robbins, Solar flares and solar wind helium enrichments: July 1965 - July 1967, *Solar Phys.*, *23*, 467, 1972*a*.

Hirshberg, J., J. R. Asbridge, and D. E. Robbins, Velocity and flux dependence of the solar-wind helium abundance, *J. Geophys. Res.*, *77*, 3583, 1972*b*,

Hirshberg, J., J. R. Asbridge, and D. E. Robbins, The helium component of solar wind velocity streams, *J. Geophys. Res.*, *79*, 934, 1974.

Howard, R. A., and M. J. Koomen, Observations of sectored structure in the outer solar corona: Correlation with interplanetary magnetic field, *Solar Phys.*, *37*, 469, 1974.

Hundhausen, A. J., *Coronal Expansion and Solar Wind*, Springer-Verlag, New York, 1972.

Hundhausen, A. J., Nonlinear model of high-speed solar wind streams, *J. Geophys. Res.*, *78*, 1528, 1973.

Hundhausen, A. J., An interplanetary view of coronal holes, in *Coronal Holes and High Speed Wind Streams*, edited by J. Zirker, p. 225, Colorado Associated University Press, Boulder, Colo., 1977.

Hundhausen, A. J., R. T. Hansen, and S. F. Hansen, Coronal evolution during the sunspot cycle: Coronal holes observed with the Mauna Loa K-coronameters, *J. Geophys. Res.*, *86*, 2079, 1981.

Jokipii, J. R., Effects of diffusion on the composition of the solar corona and the solar wind, in *The Solar Wind*, edited by R. J. Mackin and M. Neugebauer, p. 215, Pergammon, New York, 1966.

Joselyn, J. A., and T. E. Holzer, A steady three-fluid coronal expansion for nonspherical geometries, *J. Geophys. Res.*, *83*, 1019, 1978.

King, J. H., *Interplanetary Medium Data Book, Rep. NSSDC 7704*, NASA Goddard Space Flight Center, Greenbelt Md., 1977.

King, J. H., *Interplanetary Medium Data Book* (Supplement 1), *Rep. NSSDC 7908*, NASA Goddard Space Flight Center, Greenbelt, Md., 1979.

Klein, L. and L. F. Burlaga, Interplanetary sector boundaries, *J. Geophys. Res.*, *85*, 2269, 1980.

Korzhov, N. P., Large-scale three-dimensional structure of the interplanetary magnetic field, *Solar Phys.*, *55*, 505, 1977.

Krieger, A. S., A. F. Timothy, and E. C. Roelof, A coronal hole and its identification as the source of a high velocity solar wind stream, *Solar Phys.*, *29*, 505, 1973.

McIntosh, P. S., Solar magnetic fields derived from hydrogen-alpha filtergrams, *Rev. Geophys. Space Phys.*, *10*, 837, 1972.

Nakada, M. P., A study of the composition of the lower solar corona, *Solar Phys.*, *7*, 302, 1969.

Neugebauer, M., Observations of solar-wind helium, *Fundam. Cosmic Phys.*, in press, 1981.

Neugebauer, M., and C. W. Snyder, Mariner 2 observations of the solar wind, 1, Average properties, *J. Geophys. Res.*, *71*, 4469, 1966.

Newkirk, G., Structure of the solar corona, *Ann. Rev. Astron. Astrophys.*, *5*, 213, 1967.

Nolte, J. T., and E. C. Roelof, Large-scale structure of the interplanetary medium, 1, High coronal source longitude of the quiet-time solar wind, *Solar Phys.*, *33*, 241, 1973*a*.

Nolte, J. T., and E. C. Roelof, Large-scale structure of the interplanetary medium, 2, Evolving magnetic configuration deduced from multi-spacecraft observations, *Solar Phys.*, *33*, 483, 1973*b*.

Ogilvie, K. W., and T. D. Wilkerson, Helium abundance in the solar wind, *Solar Phys.*, *8*, 435, 1969.

Ogilvie, K. W., and J. Hirshberg, The solar cycle variation of the solar wind helium abundancce, *J. Geophys. Res.*, *75*, 4595, 1974.

Pneuman, G. W., The solar wind and the temperature-density structure of the solar corona, *Solar Phys.*, *28*, 247, 1973.

Pneuman, G. W., and R. A. Kopp, Gas-magnetic field interactions in the solar corona, *Solar Phys.*, *18*, 258, 1971.

Pneuman, G. W., S. F. Hansen, and R. T. Hansen, On the reality of potential magnetic fields in the solar corona, *Solar Phys.*, *59*, 313, 1978.

Robbins, D. E., A. J. Hundhausen, and S. J. Bame, Helium in the

solar wind, *J. Geophys. Res.*, *75*, 1178, 1970.
Rosenbauer, H., R. Schwenn, E. Marsch, B. Meyer, H. Miggenrieder, M. D. Montgomery, K. H. Mühlhauser, W. Pilipp, W. Voges, and S. M. Zink, A survey on initial results of the Helios plasma experiment, *J. Geophys.*, *42*, 561, 1977.
Rosenberg, R. L., and P. J. Coleman, Solar cycle-dependent north-south field configurations observed in solar wind interaction regions, *J. Geophys. Res.*, *85*, 3021, 1980.
Schulz, M., Interplanetary sector structure and the heliomagnetic equator, *Astrophys. Space Sci.*, *24*, 371, 1973.
Smith, E. J., B. T. Tsurutani, and R. L. Rosenberg, Observations of the interplanetary sector structure up to heliographic latitudes of 16°: Pioneer 11, *J. Geophys. Res.*, *83*, 717, 1978.
Svalgaard, L., J. M. Wilcox, and T. L. Duvall, A model combining the polar and the sector structured polar magnetic fields, *Solar Phys.*, *37*, 157, 1974.
Villante, U., R. Bruno, F. Mariani, L. F. Burlaga, and N. F. Ness, The shape and location of the sector boundary surface in the inner solar system, *J. Geophys. Res.*, *84*, 6641, 1979.
Wilcox, J. M., and N. F. Ness, Quasi-stationary corotating structure in the interplanetary medium, *J. Geophys. Res.*, *70*, 5793, 1965.
Wilcox, J. M., J. T. Hoeksema, and P. H. Scherrer, Origin of the warped heliospheric current sheet, *Science*, *209*, 603, 1980.
Wlérick, G., and J. Axtell, A new instrument for observing the electron corona, *Astrophys. J.*, *126*, 253, 1957.

(Received January 5, 1981;
revised April 7, 1981;
accepted April 10, 1981.